

# Aerodynamic Shaping of Spherical Turrets to Mitigate Aero-Optic Effects

Grady Crahan,<sup>1</sup> Mark Rennie,<sup>2</sup> Larry Rapagnani<sup>3</sup>, and Eric J. Jumper,<sup>4</sup>  
*University of Notre Dame, Notre Dame, IN, 46556*

and

Siviram Gogineni<sup>5</sup>  
*Spectral Energies, LLC, Dayton, OH, 45431*

**Hemispherical turrets provide an efficient means of mounting an optical system on an aircraft, but are susceptible to the formation of flows, such as shocks and separated shear layers that are known to present a severe optical aberration to the outgoing beam. In this paper, methods are presented to prevent or mitigate the formation of these aero-optic flows using improved aerodynamic shaping of the turret itself. The investigation focuses on the use of the “virtual duct” approach, which has been shown previously to successfully prevent aero-optic flows on an underwing pod up to freestream Mach numbers over 0.8. Computational fluid dynamic results are presented to demonstrate the effectiveness of the virtual duct approach, as well as other mitigation strategies.**

## Nomenclature

$C_P$	=	Pressure coefficient
$C_{P0}$	=	Pressure coefficient in incompressible flow
$C_{Pcrit}$	=	Pressure coefficient at the critical Mach number
$D$	=	Turret ball diameter
$h$	=	Fence height
$M_\infty$	=	Freestream Mach number
$M_{crit}$	=	Critical Mach number
$\gamma$	=	Ratio of specific heats (air = 1.4)
$\phi$	=	azimuthal angle
$\theta$	=	elevation angle

### Subscripts

$c$	=	Contraction portion of virtual duct
$d$	=	Diffusion portion of virtual duct

## I. Introduction

**T**HE development of airborne High-Energy Laser (HEL) systems continues to receive a high level of research effort [1]. Besides development of the laser itself, there are numerous challenges associated with integrating the HEL into the aircraft in a manner that does not degrade the performance of either the HEL system or the aircraft. In test programs and conceptual studies, the HEL is typically mounted in a spherical turret [1-5], since this

---

<sup>1</sup> Graduate Research Assistant, Center for Flow Physics and Control, AIAA Student Member.

<sup>2</sup> Research Assistant Professor, Center for Flow Physics and Control, AIAA Senior Member.

<sup>3</sup> Researcher, Center for Flow Physics and Control.

<sup>4</sup> Professor, Center for Flow Physics and Control, AIAA Fellow.

<sup>5</sup> President, AIAA Fellow.

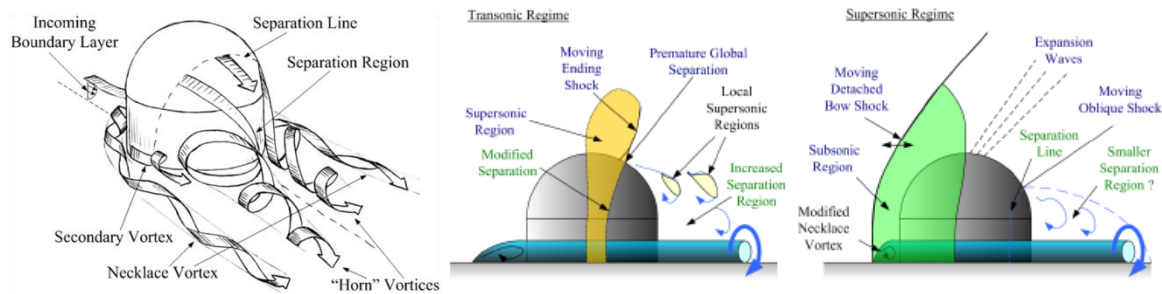


**Fig. 1. Left: Fully-subsonic flow around canonical turret; Center: Subsonic flight Mach number but transonic flow over the turret; Right: Canonical turret in supersonic flight [4].**

configuration provides ample flexibility in controlling the aiming direction of the HEL. From a flow point of view, however, spherical turrets are not ideal mounting platforms for HEL systems due to the optically-active flows that they generate which can present severe optical aberrations to the outgoing beam. For example, even in fully-subsonic flow, spherical turrets are susceptible to boundary-layer separation from their leeward surfaces, see **Fig. 1**, Left; the shear layer associated with the resulting separated flow region downstream of the turret becomes optically active in the sense that vortical structures within and without the shear layer produce severe gradients in the density and hence index of refraction [2 – 8]. It has also been shown that spherical turrets generate local supersonic flows at flight speeds that are well below typical cruise speeds for jet fighters or transport aircraft [9], see **Fig. 1**, Center; the resulting supersonic flow region terminates in a shock wave that can in and of itself seriously degrade the optical properties of a laser beam that passes through it, but also typically causes the boundary layer to separate. Aero-optic effects produced by shock waves and/or separated-flow regions present a serious limitation on the effectiveness of the HEL by restricting the field of regard of the system to directions that do not traverse optically-active flow regions.

It is therefore clear that innovative turret configurations are required that are designed from the outset to eliminate or mitigate aero-optic effects on the outgoing beam. Ideally, design of an “aero-optically optimized” turret would initially focus on pure aerodynamic solutions that do not rely on active flow-control approaches which introduce additional complexity and which could potentially fail. Furthermore, adaptive-optic (AO) correction methods should also not be the focus of initial efforts but rather, should only be used as a last resort to correct residual aberrations that remain after the best aerodynamic solution to the problem has been achieved. In this regard, it should also be noted that that shock waves may produce strong, rapidly-changing aberrations that are outside the performance envelope of current AO hardware, so that the best approach to handling shock waves may be to avoid their formation altogether. In this article, we describe our ongoing efforts to develop innovative aerodynamic approaches to optical turret designs that are tailored to eliminate or mitigate aero-optic effects on the outgoing beam.

## II. Approach

### A. Design Considerations

Based on the preceding discussion, it is clear that there is a need for innovative turret designs that avoid or at least mitigate aero-optic effects on the outgoing beam; however, any practical new turret design must also take into account the optical requirements of the outgoing beam itself. In particular, it should be noted that anti-reflective (AR) coatings typically work at only a single orientation of the outgoing beam with respect to the optical window. Furthermore, the small fraction of the outgoing beam that is reflected from the optical window and back into the turret will need to be captured using a beam dump, and it is realistic to assume that this beam dump can only be designed for a single beam orientation due to space limitations within the turret. As such, a practical turret design must assume that the outgoing beam will have a fixed orientation with respect to the optical window, so that pointing the outgoing beam must be accomplished by rotating the turret window/beam system, rather than changing the orientation of the outgoing beam within the turret itself. The need to rotate the turret to aim the beam further

supports the use of rotationally-symmetric shapes (i.e. cylindrical or spherical), at least in the region where the optical window is located, since these shapes can be rotated without altering the basic aerodynamics of the turret.

It is therefore apparent that traditional turret shapes like the hemispherical turret offer significant advantages in terms of aiming the outgoing beam as well as satisfying optical constraints for projecting the beam out of the turret in the first place. On the other hand, spherical turrets are not ideal shapes for avoiding aero-optic flows. Specifically, in inviscid, incompressible flow, the minimum pressure coefficient,  $C_{p0}$ , on a sphere is -1.25 [9, 10], which has been experimentally validated for the case of a hemispherical turret on a  $D/3$  cylindrical base [4] ( $D$  is the hemisphere diameter). These  $C_{p0}$  values can be corrected for compressibility effects using, for example, the Karman-Tsien formula [11]:

$$C_p = \frac{C_{p0}}{\sqrt{1 - M_\infty^2} + \left( \frac{M_\infty^2}{1 + \sqrt{1 - M_\infty^2}} \right) \frac{C_{p0}}{2}}. \quad (1)$$

As the freestream  $M_\infty$  increases, the maximum local flow speed will eventually become sonic (even for  $M_\infty < 1$ ); the freestream Mach number at which this occurs is called the critical Mach number,  $M_{crit}$ , and the local  $C_p$  required for this to happen is called the critical  $C_p$ ,  $C_{p_{crit}}$ .

$$C_{p_{crit}} = \frac{2}{\gamma M_{crit}^2} \left[ \left( \frac{1 + \frac{\gamma - 1}{2} M_{crit}^2}{1 + \frac{\gamma - 1}{2}} \right)^{\frac{\gamma}{\gamma - 1}} - 1 \right]. \quad (2)$$

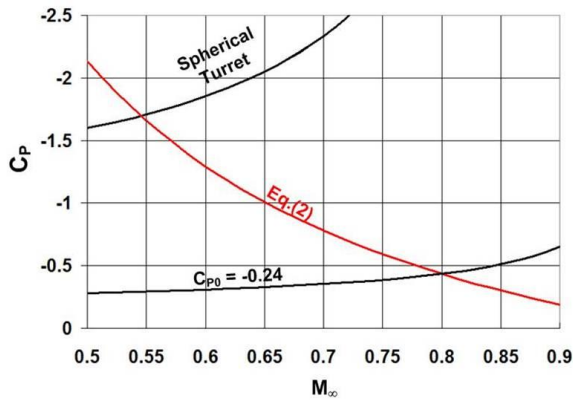


**Fig. 2. Critical Mach number for hemispherical turret, and minimum  $C_{p0}$  to avoid shock formation during cruise at  $M_\infty = 0.8$  [9].**

itself. This means that strategies such as reducing the height of the exposed portion of the hemisphere to present only a “blister” to the oncoming flow has only a minimal effect in increasing the critical Mach number.

Besides a relatively low critical Mach number, hemispherical turrets are also susceptible to boundary-layer separation from the aft surface of the turret which occurs at an angle of approximately  $120^\circ$  from the direction of the oncoming flow [4]. At compressible flow speeds, the shear layer associated with this separated flow region becomes optically active and can seriously degrade the ability to focus an outgoing beam on targets in the farfield [6-8]. In summary, the goal of mitigating aero-optic effects means that the objectives should be to increase the critical Mach number to reasonable flight Mach numbers typical of transonic platforms of interest, and to prevent or delay flow separation on the aft portion of the turret.

The intersection of these two curves, **Error! Reference source not found.**, shows that supersonic flow occurs on a spherical turret at a freestream Mach number just below  $M_\infty = 0.55$ ; this Mach number is significantly below the nominal  $M_\infty \approx 0.8$  to  $0.89$  cruise speed of jet transports and combat aircraft. Instead, **Error! Reference source not found.** shows that in order to achieve a critical Mach number of 0.8 (barely sufficient for jet aircraft cruise), the minimum  $C_{p0}$  can be no less than -0.24. Once the local flow speed exceeds a Mach number of 1.0, a shock will form downstream of the supersonic-flow region, hence the term, “critical Mach number.” The strong density and hence index-of-refraction variation across the shock wave would present a serious optical aberration to an outgoing beam that traversed the shock; furthermore, the unsteady motion of the shock would make it difficult to correct using an adaptive-optic approach.

It should be noted that the low critical Mach number of  $M_{crit} = 0.55$  for the canonical hemispherical turret is caused primarily by the high curvature of the turret

## B. The “Virtual Duct” Concept

Our previous investigations into aero-optic optimization of turret configurations are described in [9, 10], which detail our efforts to prevent or mitigate aero-optic aberrations around a laser pod designed to be carried under the wing of a fighter aircraft. The approach used to mitigate aero-optic aberrations in the vicinity of the optical aperture relied partially upon streamlining the pod shape to delay supersonic flow speeds and hence shock formation around the optical aperture up to high subsonic freestream Mach numbers,  $M_\infty$ . The bulk of the performance gain was achieved, however, by placing fences on the spherical turret ball at the nose of the pod that were shaped to favorably modify the flow around the optical aperture. In particular, the fences were shaped to diffuse the flow over the front of the turret ball, thereby reducing the maximum flow speed over the turret ball and delaying the freestream Mach number at which shocks form. At the same time, the fences were shaped to accelerate the flow on the rear of the turret ball to prevent flow separation in this region. In effect, the fences, and the surface of the turret ball itself form a “virtual duct” which is shaped to control the flow around the optical aperture of the outgoing beam.

Figure 3, Left, shows a schematic of the virtual duct concept applied to an underwing pod; note the modified aiming dynamics in the sense that the optical aperture moves between the fences of the virtual duct while the entire nose section of the pod rotates in a “roll shell” that keeps the fences of the virtual duct aligned with the oncoming flow. Figure 3, Right, shows both experimental and CFD results that show reduced flow speeds and a reduced adverse pressure gradient on the turret ball, thereby validating the virtual-duct approach.

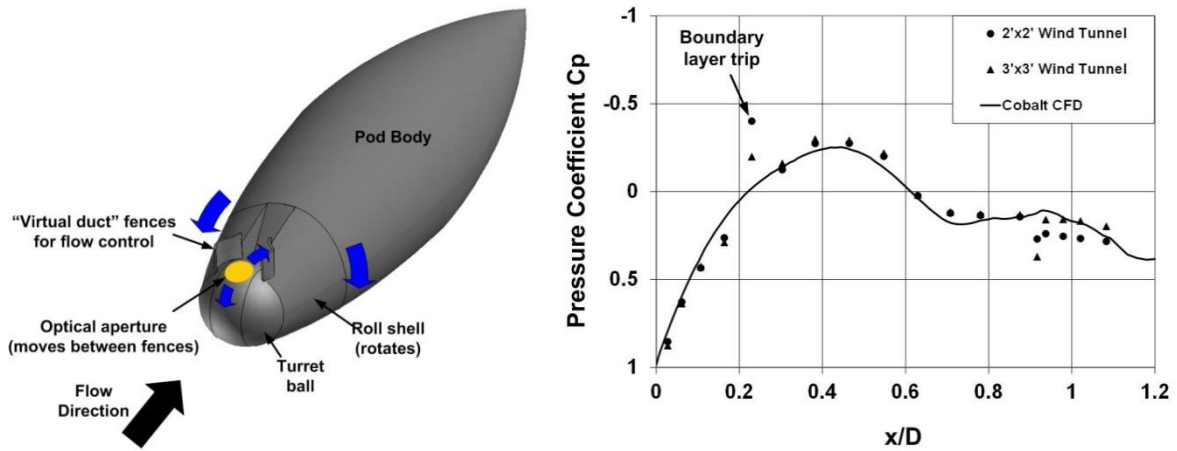


Fig. 3. Schematic (left) of aero-optic pod concept showing virtual duct approach to controlling flow in the vicinity of the optical aperture, and comparison (right) of measured and computed pressures on the pod [10].

## III. Results

### A. The Virtual Duct Concept Applied to a Hemispherical Turret

Based on the success of the virtual duct concept in preventing the formation of aero-optic flows around an underwing laser pod, the virtual-duct concept was next tested on a canonical hemispherical turret configuration. For this study, the virtual-duct wall coordinates for the model were determined using fifth-order polynomials for both the diffusing section on the upstream part of the turret and the contracting section on the downstream part of the turret:

$$\begin{aligned}
 y_d &= a_d + b_d x + c_d x^2 + d_d x^3 + e_d x^4 + f_d x^5 \\
 y_c &= a_c + b_c x + c_c x^2 + d_c x^3 + e_c x^4 + f_c x^5
 \end{aligned}
 \tag{3}$$

where  $y_d$  and  $y_c$  are the locations of the virtual-duct fence on the turret ball surface for the diffusing and contracting sections respectively. The six constants  $a, b, c, \dots, f$  for each section were determined by the six boundary conditions

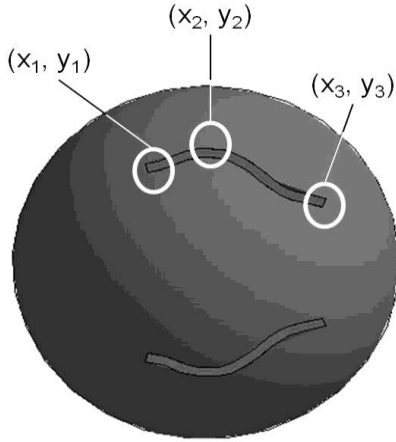


**Fig. 4. Schematic of the three points used to define the fence, (1) the leading edge, (2) the point of maximum diffusion of the fence and, (3) the trailing-edge point.**

The near optimum turret configuration from this study is shown in Fig. 5. Note that for this initial study, the fence height  $h$  from the bottom of the turret base to the top of the fence (see Fig. 5) was set at  $1.2 D$ , and the maximum downstream extent of the virtual-duct fences was limited to  $x_3 = 0.85 D$ . The computed pressure distribution along the turret centerline for this configuration is shown in Fig., Right, and shows the improvements made by adding the virtual duct, specifically, a large reduction in the peak  $-C_{p0}$  (i.e. increase in the critical Mach number) and a reduction in the adverse pressure gradient on the rear of the turret. Using Eqs. **Error! Reference source not found.** and **Error! Reference source not found.**, the critical Mach number for the turret with the virtual duct was determined to be  $M_{crit} = 0.74$ , considerably greater than the unfenced turret with a  $M_{crit} = 0.55$ .

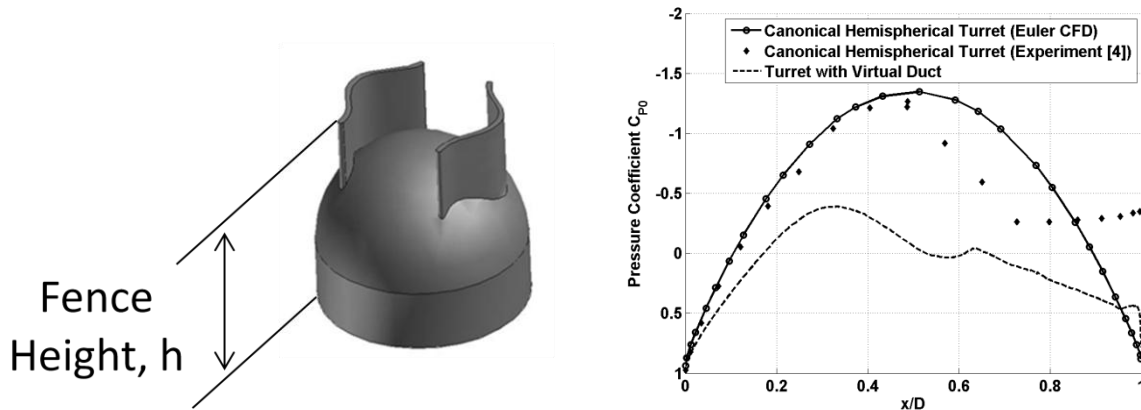


**Fig. 5. Left: Diagram of turret with virtual duct. Right: Improvement in pressure distribution produced by virtual duct with fence height,  $h$ , of  $1.2D$  above the bottom of the base of the turret. The critical Mach number for the shown configuration is  $M_{crit} = 0.74$ .**

The results presented up to this point have for the most part shown how the virtual duct can improve the critical Mach number of a hemispherical turret. To more fully illustrate how the virtual duct can also delay boundary-layer separation on a hemispherical turret, the flow over the turret was also computed using a Reynolds-Averaged Navier Stokes (RANS) code. Figure 6 Left shows that the RANS solution for the unmodified turret accurately predicts flow

consisting of the chosen starting and ending azimuthal locations of the fence, plus zero slope and curvature at the start and end of each section of the fence. As such, a unique fence shape can be defined by choosing the locations of three points on the fence, consisting of the leading- and trailing-edge points and the point of maximum diffusion of the fence, see Fig. 4.

Using the above approach, a large number of different virtual-duct shapes were evaluated using CFD to find a near-optimum shape that both maximized the critical Mach number while reducing the adverse pressure gradient on the turret. Since the objective of the virtual-duct approach is to delay or prevent boundary-layer separation on the rear of the turret and therefore create an inviscid-like flow around the turret, this initial screening of virtual-duct fence shapes was performed using an Euler code, and the best shapes from this initial screening were further studied using full Navier-Stokes simulations. The computations were also run at a relatively low Mach number, and the resulting computed pressure distributions on the turret were used to determine the critical Mach number using Eqs. (1) and (2) above.

separation at an angle of approximately  $119^\circ$  with respect to the oncoming flow, which is in agreement with experimental studies for turbulent-flow separation from canonical turret configurations [4]. Figure 6 Right plots the flow vorticity for the same turret modified with the virtual duct shown in Fig. 5; in this case, the virtual duct delays flow separation from the turret up to an angle of  $138^\circ$  with respect to the oncoming flow. It is interesting to note that the location of flow separation corresponds very closely to the trailing edge of the virtual duct; furthermore, the centerline pressure distribution for this configuration, shown in Fig. 5 (right), also shows a small peak at this location. As such, these results indicate that it should be possible to delay boundary layer separation on the turret to even larger angles simply by extending the trailing edge of the virtual-duct fences further aft on the turret.

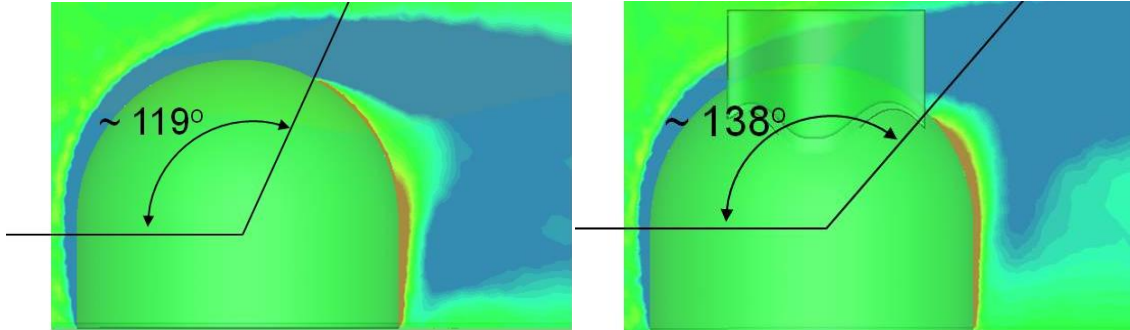


**Fig.6. CFD-computed vorticity contours around a canonical hemispherical turret (left) and a turret with virtual duct (right), showing that the virtual duct delays boundary layer separation by an additional  $\sim 20^\circ$  with respect to the oncoming flow direction.**

## B. Further Improvement Strategies

One way to further improve the performance of the turret (i.e. raise the  $M_{crit}$  and delay flow separation) would be to increase the height of the virtual duct; this was shown to have a significantly beneficial effect on  $M_{crit}$  in previous design studies of the aero-optic pod [9, 10]. On the other hand, a higher virtual-duct fence height might lead to other problems such as an increase in unsteady aerodynamic forces and moments on the turret that could lead to aerodynamically-induced jitter of the turret, or possibly even structural issues.

### 1. Fairings

The performance of the turret could also be improved using fairings. In this case, the fairings would be designed to “blend in” to the surface of the spherical turret, thereby reducing the curvature of the turret (i.e. streamline the turret) producing lower local flow speeds over the turret and hence a higher critical Mach number. As shown in [9], however, in order to streamline the spherical turret enough to attain  $M_{crit} \approx 0.8$ , a downstream fairing would have to blend in to the turret at a point on the upstream half of the turret ball, so that the fairing would obscure much of the field of regard out of the turret. This could be rectified using some kind of control strategy that would move the fairing out of the way of the outgoing beam as the aiming direction of the turret changes. Alternately, an approach similar to the aero-optic pod shown in Fig. 3 could be taken, in which a cutout is made in the downstream fairing so that the beam can be directed at targets in the aft field of regard; in effect, the turret in this case would look like the upper half of the full pod shown in Fig. 3. Note that in [9, 10] it was shown that this kind of configuration could achieve  $M_{crit}$  values of over 0.8, although the aft field of regard was limited to a maximum aiming direction of  $40^\circ$  past vertical.

### 2. Outer Fences

Besides using fairings, another possible approach to improving the turret performance would be to attempt to reduce the flow speed at the location of the turret as a whole. This could be accomplished by strategically locating the turret at a point on the aircraft where flow speeds are reduced. Alternatively, the turret could be placed inside a carefully shaped shallow cavity in the aircraft. As a first attempt at modeling this kind of arrangement, CFD solutions were computed for configurations in which the turret was placed inside a second set of fences that now surrounded the entire turret. For these initial simulations, the outer fences were modeled in a similar manner as the

virtual duct on the turret itself; that is, the outer fences were shaped to diffuse the flow reaching the turret and then to reaccelerate the flow around the back of the turret

A typical CFD model used to model the effect of placing the turret in a cavity is shown in Fig. 7. The pressure distribution in **Error! Reference source not found.**, Right, shows how this particular configuration further improves the pressure distribution on the turret in the sense that it further reduces the suction peak on the turret (i.e. increases the  $M_{crit}$ ) and reduces the pressure gradient on the rear of the turret. The critical Mach number for the configuration shown in Fig. 7 is  $M_{crit} = 0.82$ . Note that other configurations such as shown in Fig. 7 were also investigated that could actually raise the critical Mach number to almost 1.0; however, the outer fence in this case was higher than the turret, and so would itself present a significant obscuration to the outgoing beam.

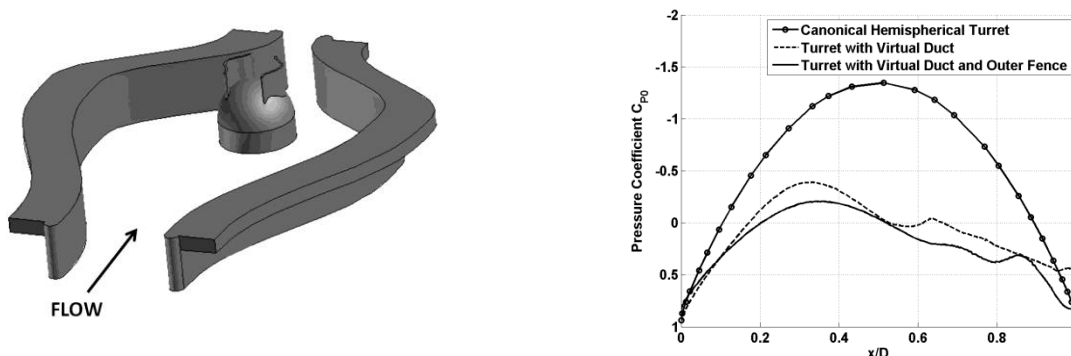


**Fig.7. Left: Schematic of turret with virtual duct located in a region of reduced flow speed produced by, for example, a shaped cavity. Right: Improvement in pressure distribution along the turret centerline due to the virtual duct and combined virtual duct with outer fences.**

The outer fence configuration shown in Fig. 7 is only an initial representation of a possible approach to increasing the  $M_{crit}$  by slowing the overall flow that reaches the turret, and additional development of the concept is necessary. On the other hand, the outer fence configuration also revealed another possible aerodynamic approach to controlling the flow over the turret. In particular, it was found that at freestream Mach numbers greater than approximately  $M_\infty \sim 0.7$ , the flow entering the outer fences accelerated to sonic speed and then shocked just downstream of the inlet to the outer fences. The effect of this shock is shown in Fig. 8, which shows the computed minimum  $C_p$  on the turret as a function of incoming freestream Mach number. Note that the data shown in Fig. 8 were computed using a canonical hemispherical turret that did not have a virtual duct installed. Figure 8 shows that the effect of the upstream shock is to shift the  $C_p$  curve so that the critical Mach number on the turret occurs at a higher freestream Mach number. In effect, the upstream shock reduces the speed of the flow approaching the turret. As such, although the outer fence configuration shown in Fig. 7 is only an initial concept, it illustrates the possibility of using an upstream shock to further diffuse the flow reaching the turret; as shown in the next section, this result may have a particularly beneficial impact on turret designs at supersonic freestream Mach numbers.

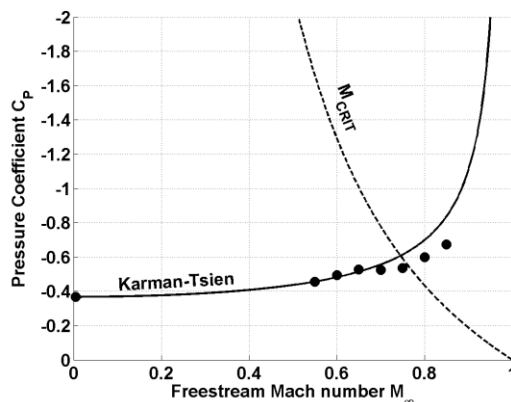


**Fig. 8. Minimum  $C_p$  on turret as a function of  $M_\infty$  for a canonical turret with outer fences. The shift in the CFD data (dots) at  $M_\infty \approx 0.65$  shows that the flow reaching the turret is slowed by an upstream shock.**

### C. Supersonic Flow

At supersonic freestream Mach numbers, it must be accepted that a shock wave(s) will exist in the vicinity of the turret. Whereas in transonic flight the shock forms on the turret, in supersonic flight the shock forms in front of the turret as a bow shock (see

**Fig. 1, Right**). This shock wave would present a serious optical aberration to any beam that passes through it, and further investigations into the optical effects of shocks as well as mitigation strategies are needed.

Although the bow shock would present a serious optical aberration for forward aiming directions of the outgoing beam, as shown in the preceding section, the upstream bow shock could also have a beneficial effect by slowing down the flow in the immediate vicinity of the turret. A CFD solution, run at a freestream Mach number of  $M_\infty = 1.3$  is shown in Figs. 9 and 10, and demonstrates exactly this kind of behavior. Specifically, the figures show that the incoming flow forms an initial bow shock ahead of the inlet, then accelerates again to sonic, and then shocks again in the throat of the outer fences. Downstream of this second shock, the flow then remains subsonic around and over the turret except in small pockets of flow outside the duct walls. In particular, a close-up view of the local Mach number distribution on the surface of the turret (Fig. 10, Right) shows that the flow remains fully subsonic around the turret and that no shocks form on the turret itself. As such, although it is clear that a beam projected forward would still have to contend with propagation through a shock wave(s); there appears to be large regions of the field of regard that would allow laser propagation without encountering a shock. Furthermore, flow solutions that would keep the flow attached to the turret at subsonic freestream Mach numbers would continue to work for the supersonic  $M_\infty$  case shown in Figs. 9 and 10 because the flow in the immediate vicinity of the turret is fully subsonic. It should be mentioned again that the outer fence configuration used in this part is just an initial concept and that the same kind of “shock diffusion” illustrated in Figs. 9 and 10 could potentially be achieved using other shapes, or by careful integration of the turret into the already-existing flowfield of the transporting aircraft.

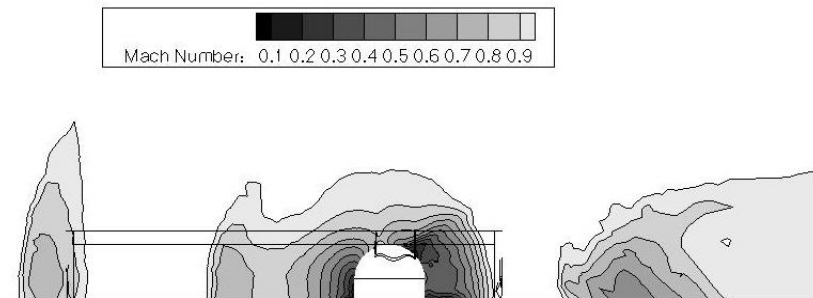


**Fig. 9. Mach number distribution in zenith plane around turret with virtual duct surrounded by outer fence configuration such as shown in Fig. 7, for  $M_\infty = 1.3$ . Flow is from left to right; note shock at the inlet of the outer duct.**

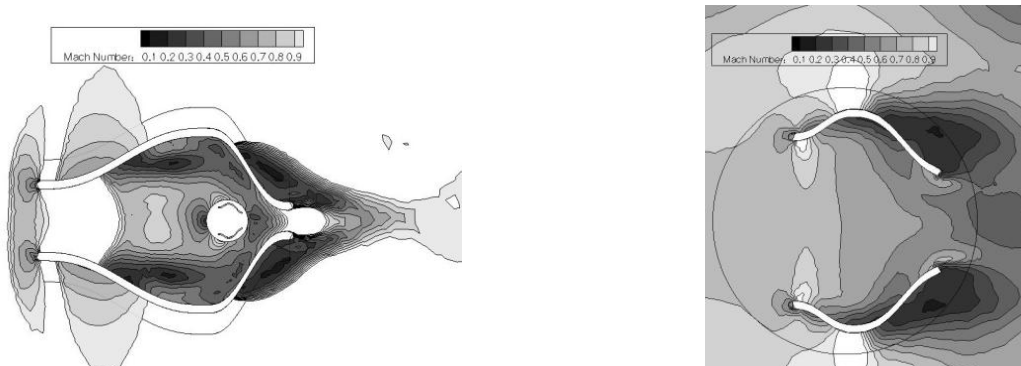


**Fig. 10. Left: Mach number distributions in plain view corresponding to Fig. 9; Right: Closeup view of local Mach number distribution just above the surface of the turret.**

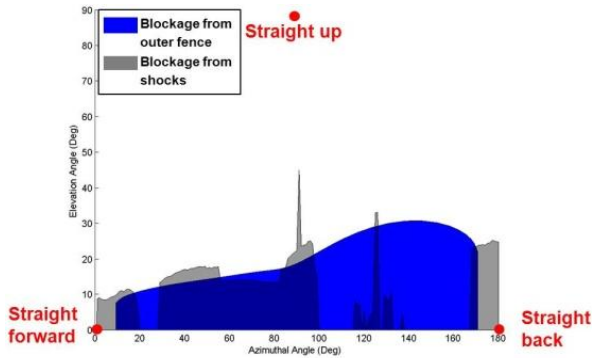


**Fig. 11. Field of regard of turret with virtual duct and outer fence configuration, showing elevation and azimuth aiming angles that are unaffected by aero-optic flows or structures.**

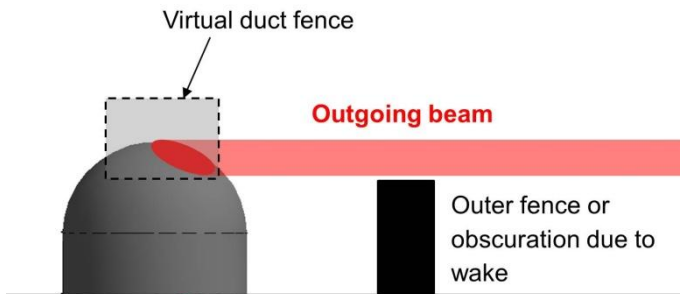


**Fig. 12. Improvement in field of regard of turret that is realized by raising the outgoing beam.**

results have shown that the critical Mach number for a hemispherical turret with virtual duct can be increased to around  $M_{crit} \sim 0.74$ , which is significantly higher than the  $M_{crit}$  of 0.55 for a canonical hemispherical turret. The critical Mach number could be improved still further, to above a Mach number of 0.8, using either fairings or by slowing the oncoming flow to the turret using, for example, an outer fence arrangement. Furthermore, at high transonic and supersonic freestream Mach numbers, it should be possible to use the upstream shock to “shock-diffuse” the flow, thereby keeping the turret entirely in subsonic flow so that the primarily subsonic design methods illustrated in this paper would continue to work for  $M_\infty > 1$ . It should be noted that the virtual-duct configurations shown here were by no means fully optimized, so that it is likely that even better performance than given above can be achieved.

The CFD results also showed that the virtual duct successfully delays flow separation from the turret. Viscous CFD data showed that the virtual duct delayed separation from 119° on a turret with no duct, to 138° on a turret with a virtual duct. However, the point of flow separation on the turret with the virtual duct corresponds to the trailing edge of the virtual duct, so that it is likely that flow separation could be delayed still further by extending the virtual duct fences further aft. Finally, in all cases considered, the field of regard of the turret could be improved still further by mounting the window for the outgoing beam in a raised position on the turret.

#### D. Field-of Regard

Optical aberrations from shock waves and/or compressible shear layers present a limitation on the effective field of regard of the aircraft-mounted optical system, in the sense that they limit the range of aiming angles at which the outgoing beam will produce an effective irradiance on target. A typical field-of-regard plot for a turret with virtual and outer fence configuration is shown in Fig. 11.

One approach to further improving the field of regard of the turret would be to change the angle at which the beam emerges from the turret such as shown in Fig. 12. Note that for the case shown in Fig. 12, the outgoing beam would still be aimed by rotating the turret, and that the orientation of the outgoing beam with respect to the window on the turret would still remain fixed thereby satisfying optical-coating and beam-dump constraints discussed above. In effect, the beam orientation shown in Fig. 12 lifts the beam higher above any obstructions to the field of regard of the optical turret. Note that this beam orientation also makes the turret with virtual duct solution more tractable, since it would also “lift” the outgoing beam above the separated flow region on the back of the turret, as depicted in Fig. 6, Right.

#### IV. Summary

The results of this CFD study have shown that the virtual-duct approach can be used to successfully mitigate aero-optic flows on a hemispherical turret. In particular, these initial

## Acknowledgements

These efforts were sponsored by the Air Force SBIR (Small Business Innovative Research) Program under Award Number FA8650-11-M-3115. The authors acknowledge the support of Mr. Donnie Saunders of AFRL. The U.S. Government is authorized to reproduce and distribute reprints for governmental purposes notwithstanding any copyright notation thereon.

## References

- [1] Horkovitch, J.A., "Directed Energy Weapons: Promise and Reality," AIAA Paper 2006-3753, June, 2006.
- [2] Gordeyev, S., Hayden, T., and Jumper, E., "Aero-Optical and Flow Measurements over a Flat-Windowed Turret," *AIAA Journal*, Vol. 45, No. 2, 2007, pp.347-357.
- [3] Gordeyev, S., Post, M.L., McLaughlin, T., Ceniceros, J., and Jumper, E.J., "Aero-Optical Environment Around a Conformal-Window Turret," *AIAA Journal*, Vol. 45, No. 7, 2007, pp.1514-1524.
- [4] Gordeyev, S. and Jumper, E.J., "Fluid Dynamics and Aero-Optical Environment Around Turrets," AIAA Paper 2009-4224, June, 2009, (To appear in *Prog. Aero. Sci.*)
- [5] Vukasinovic, B., Glezer, A., Gordeyev, S., Jumper, E., and Kibens, V., "Active Control and Optical Diagnostics of the Flow over a Hemispherical Turret," AIAA Paper 2008-0598, Jan., 2008.
- [6] Jumper, E.J., and Fitzgerald, E.J., "Recent advances in aero-optics," *Progress in Aerospace Sciences*, Vol. 37, 2001, pp. 299-339.
- [7] Fitzgerald, E.J. and Jumper E.J., "The optical distortion mechanism in a nearly incompressible free shear layer," *Journal of Fluid Mechanics*, Vol. 512, 2004, pp. 153-189.
- [8] Rennie, R.M., Duffin, D.A., and Jumper, E. J., "Characterization and Aero-Optic Correction of a Forced Two-Dimensional, Weakly-Compressible Subsonic Free Shear Layer," *AIAA Journal*, Vol. 46, No. 11, 2008, pp.2787-2795.
- [9] Rennie, R. M., Crahan, G., and Jumper, E. J., "Aerodynamic Design of an Aircraft-Mounted Pod for Improved Aero-Optic Performance," AIAA Paper 2010-0437, Jan, 2010
- [10] Crahan, G., Rennie, R.M., and Jumper, E.J., "Experimental Measurements of an Aircraft-Mounted Pod Concept for Improved Aero-Optic Performance," AIAA Paper 2011-1329, Jan. 2011.
- [11] Anderson, J.D., *Modern Compressible Flow, 3<sup>rd</sup> Ed.*, McGraw Hill, New York, 2003.